energy&fuels

ARTICLE

pubs.acs.org/EF

Measurement and Prediction of Biodiesel Surface Tensions

Samuel V. D. Freitas,[†] Mariana B. Oliveira,[†] António J. Queimada,[‡] Maria Jorge Pratas,[†] Álvaro S. Lima,[§] and João A. P. Coutinho*[,†]

[†]Centre for Research in Ceramics and Composite Materials (CICECO), Department of Chemistry, University of Aveiro, Campus de Santiago, 3810-193 Aveiro, Portugal

[‡]Laboratory of Separation and Reaction Engineering (LSRE), Faculdade de Engenharia, Universidade do Porto, 4200-465 Porto, Portugal

[§]Universidade Tiradentes, Avenida Murilo Dantas 300, Farolândia, 49032-490 Aracaju, Sergipe (SE), Brazil

ABSTRACT: Surface tension is one of the key properties that directly affects fuel atomization. A large value of this property makes the formation of small droplets difficult, hampering the correct fuel atomization on the engine combustion chamber. Despite its importance, there are very few data on the surface tension of biodiesels or fatty acid esters from which biodiesels are composed and even less are available on its temperature dependence. To overcome this limitation, this work reports experimental surface tensions for 10 biodiesel fuels in a wide temperature range and evaluates the ability of two models to predict these data: the parachor-based MacLeod−Sugden equation and the density gradient theory based on the cubic-plus-association equation of state (CPA EoS). It is shown that both models provide an acceptable description of the experimental surface tension of the biodiesel fuels studied, with an overall average relative deviation (OARD) of 7.7% for the MacLeod−Sugden equation using the Allen's parachors and 1.3% with the Knotts' parachors, while the CPA EoS combined with the gradient theory presents an OARD of 9.7%. The surface entropy and enthalpy derived from the measured surface tensions are also reported, and their values indicate the importance of the surface ordering in biodiesel fuels. Given the scarcity of data on surface tensions, these models prove to be useful for predicting surface tensions and their temperature dependence for biodiesel fuels.

1. INTRODUCTION

In what concerns energy and fuel policies, governments and international organizations have focused on the importance of biodiesel fuels. The idea is that these fuels may allow for countries to take advantage of their proven benefits for energy sustainability and environmental protection. With their use, mankind can be able to reduce its dependency upon fossil fuels, which are already in decline and have a huge negative impact on the environment because of the emission of aggressive greenhouse gases during combustion.[1] Neat biodiesel (B100) can reduce carbon dioxide emissions (CO_2) by more than 75% over petroleum diesel, while a B20 reduces CO_2 by 15%.[2,3] Only NO_x emissions increase about 10−15% in comparison to that of petrodiesel, because biodiesel contains 10−11% oxygen.[4−6]

Biodiesel, a mixture of fatty acid monoalkyl esters, is obtained by transesterification of vegetable oils, animal fats, or used frying oils, with short-chain alcohols, such as methanol or ethanol, in the presence of a catalyst.[7−9] As a fuel, it offers more benefits than damages in comparison to petroleum-based fuels, because it is economically competitive (domestically produced), environmentally friendly (biodegradable, renewable, and producing less harmful emissions),[2,10−18] and mixable with petrodiesel at any proportion to be used in diesel engines with almost no modification.[9,17,19−21]

To enhance biodiesel quality, however, its physical properties require severe control to be consistent with the requirements established by the quality standards ASTM D6751[22] in the United States and EN 14214[23] in Europe.

Because biodiesel properties strongly depend upon the fatty acid profiles of the feedstocks, they can be tuned using raw materials containing components that will provide more favorable properties to biodiesels. For that purpose, an accurate knowledge of the most important biodiesel and fatty acid ester properties must be acquired. In previous works, we have been addressing some of these properties for several biodiesels and their pure components, such as density,[24−26] viscosity,[27−29] speed of sound,[30] water content,[31] and low-temperature behavior.[32−35]

In this work, surface tensions are addressed. This property has a major impact on fuel atomization, i.e., the first stage of combustion.[9] A correct atomization allows for proper mixing and complete combustion in an injection engine, reducing emissions and increasing the engine efficiency.[36] Higher surface tensions make the drop formation difficult, leading to an inefficient fuel atomization.[36] Furthermore, just like most biodiesel properties, surface tension increases with long fatty acid hydrocarbon chains and a level of unsaturated bonds;[37] i.e., more unsaturated biodiesel fuels will present a higher surface tension. Thus, being able to predict this physical property for biodiesels for which composition on fatty acid esters is known makes it possible to optimize biodiesel production and blending processes, with the final aim of improving the fuel performance in the engine, particularly during atomization.

Received: August 10, 2011
Revised: September 15, 2011
Published: September 19, 2011

Table 1. Compositions of the Biodiesels Studied, in Mass Percentage and Parachors of Pure FAMEs

FAMEs	Allen's parachors[38]	Knotts' parachors[45]	Soy B	R	P	SR	RP	SP	SRP	Sf	GP	Soy A
C10	489	495		0.01	0.03		0.02	0.01	0.01			
C12	567	574		0.04	0.24	0.03	0.20	0.18	0.14	0.02	0.02	
C14	645	657	0.07	0.07	0.57	0.09	0.54	0.01	0.38	0.07	0.13	
C16	723	737	10.76	5.22	42.45	8.90	23.09	25.56	19.07	6.40	10.57	16.18
C16:1	712	726	0.07	0.20	0.13	0.15	0.17	0.11	0.14	0.09	0.13	
C18	801	817	3.94	1.62	4.02	2.76	3.02	4.04	3.30	4.22	2.66	3.82
C18:1	879	806	22.96	62.11	41.92	41.82	52.92	33.13	42.74	23.90	41.05	28.80
C18:2	779	795	53.53	21.07	9.80	37.51	15.47	31.72	28.08	64.16	36.67	50.46
C18:3	768	782	7.02	6.95	0.09	7.02	3.08	3.58	4.68	0.12	7.10	
C20	879	897	0.38	0.60	0.36	0.46	0.49	0.39	0.46	0.03	0.44	
C20:1	868	886	0.23	1.35	0.15	0.68	0.67	0.20	0.53	0.15	0.67	
C22	957	978	0.80	0.35	0.09	0.46	0.24	0.32	0.33	0.76	0.45	
C22:1	946	967	0.24	0.19	0.00	0.12	0.09	0.12	0.15	0.08	0.12	
C24	1035	1058		0.22	0.15			0.63				

There is, however, a lack of information concerning surface tensions of biodiesels or fatty acid esters from which biodiesels are composed, and when available, the data are limited to a single temperature.[37,38] To overcome that lack of data, this work provides experimental surface tension data for 10 different biodiesel fuels. The experimental data were acquired at temperatures from 303.15 to 353.15 K. The data were used to test two surface tension predictive models: the parachor-based MacLeod−Sugden equation and the density gradient theory based on the cubic-plus-association equation of state (CPA EoS).

2. EXPERIMENTAL SECTION

With the exception of two biodiesel fuels, soybean (Soy A) and soybean + rapeseed (GP), that were obtained from Portuguese biodiesel producers (Prio and Galp, respectively), the other eight biodiesel fuels studied here were synthesized at our laboratory, as described in a previous work,[24] by the transesterification reaction of the following vegetable oils with methanol: soybean (Soy B), rapeseed (R), and palm (P) and their respective binary and ternary mixtures: soybean + rapeseed (SR), rapeseed + palm (RP), soybean + palm (SP), and soybean + rapeseed + palm (SRP), and sunflower (Sf). Their compositions are reported in Table 1.[24]

The measurement of the surface tension of the biodiesel samples was carried out using a Nima dynamic surface tensiometer, model DST9005, previously used for studies of hydrocarbon mixtures[39−41] and ionic liquids.[42−44] This is a sophisticated computer-controlled instrument that measures and records the forces that biodiesel exerts to withstand the external force provoked by the immersion of the Pt/Ir Du Noüy ring in the liquid. A Haake F6 bath circulator, equipped with a Pt100 probe, was connected to the tensiometer to guarantee that measurements occurred within an uncertainty of ±0.01 K. The ring was always cleaned before each measurement in a butane flame. The measurement was carried from 303.15 to 353.15 K for all biodiesel fuels. For each sample, at least five sets of three immersion/detachment cycles were measured, providing a minimum of at least 15 surface tension values, allowing for the determination of an average surface tension value for each temperature. To correct the meniscus formed by the Noüy ring, the liquid densities of the biodiesels reported in a previous work[24] were introduced before measuring the surface tension.

3. PREDICTION OF BIODIESEL SURFACE TENSIONS

The surface tensions of the biodiesel fuels studied here were predicted using two different predictive approaches: the parachor-based MacLeod−Sugden equation with the parachors proposed by Allen et al.[38] and Knotts et al.[45] and the density gradient theory based on the CPA EoS.[46−48]

The first model requires prior knowledge of densities and molar masses of biodiesel fuels according to eq 1

$$\gamma = \left(\frac{P_{ch}\rho}{M_w}\right)^4 \quad (1)$$

where γ is the surface tension in N m^{-1}, ρ is the density in g cm^{-3}, P_{ch} is the parachor in $((\text{mN m}^{-1})^{1/4})/\text{cm}^3\ \text{mol}^{-1}$, and M_w is the molar mass in g mol^{-1}. The densities of the biodiesel fuels were already reported in a previous work.[24] The parachors for the biodiesels were calculated from the parachors of pure fatty acid methyl esters (FAMEs) presented in Table 1 using the mixing rules of eq 2

$$P_{ch}\text{BDF} = \sum_i (x_i P_{ch} i) \quad (2)$$

where P_{ch}BDF is the parachor of the biodiesel and x_i and $P_{ch}i$ are the molar fraction and the parachor of pure FAMEs, respectively. A similar mixing rule was also used to estimate the molar mass of biodiesel fuels.

The gradient theory is based on the phase equilibria of the fluid phases separated by an interface.[49,50]

$$\gamma = \int_{n^{vap}}^{n^{liq}} \sqrt{2c\Delta\Omega(n)\sum_i\sum_j c_{ij}\frac{\partial n_i}{\partial n_N}\frac{\partial n_j}{\partial n_N}}\, \mathrm{d}n_N \quad (3)$$

$$\Delta\Omega(n) = f_0(n) - \sum_i n_i\mu_i + p \quad (4)$$

where p is the equilibrium pressure, γ is the surface tension, $f_0(n)$ is the Helmholtz energy density of the homogeneous fluid, μ_i values are the pure-component chemical potentials, n^{liq} and n^{vap} are the liquid and vapor phase molar densities, respectively, and c is the so-called influence parameter.

Table 2. Experimental Surface Tensions for Biodiesel Fuels, in mN m^{-1}

T (K)	Soy B	σ^a	R	σ	P	σ	SR	σ	RP	σ	SP	σ	SRP	σ	Sf	σ	GP	σ	Soy A	σ
303.15	31.71	0.23	32.18	0.08	31.89	0.03	31.64	0.06			31.27	0.04	31.53	0.01			31.57	0.01	30.89	0.55
313.15	30.56	0.05	31.17	0.45	30.55	0.00	30.52	0.03	30.74	0.03	30.47	0.03	30.49	0.03	31.15	0.09	30.55	0.23	29.74	0.38
323.15	29.45	0.21	30.14	0.01	29.86	0.01	29.46	0.01	29.70	0.01	29.70	0.02	29.40	0.08	29.39	0.16	29.54	0.27	28.66	0.06
333.15	28.16	0.04	28.60	0.04	28.62	0.03	27.90	0.22	28.50	0.00	28.76	0.06	28.56	0.05	28.29	0.02	28.50	0.22	27.98	0.05
343.15	27.40	0.02	27.39	0.29	27.84	0.01	27.14	0.76	27.71	0.39	27.68	0.03	27.29	0.01	27.47	0.17	27.59	0.09	26.97	0.13
353.15	26.68	0.03			26.62	0.07	26.22	0.20	26.89	0.04	26.68	0.04	26.07	0.02	26.04	0.19	26.57	0.02	25.97	0.10

[a] σ = standard deviation.

The theoretical definition of the pure-component influence parameter, c, can hardly be implemented, as an alternative, after the vapor−liquid equilibrium is determined. This parameter is frequently correlated from surface tension data.

$$c = \frac{1}{2}\left[\frac{\gamma_{\exp}}{\int_{n^{\mathrm{vap}}}^{n^{\mathrm{liq}}} \sqrt{f_0(n) - n\mu + p}\,\mathrm{d}n}\right]^2 \tag{5}$$

To use the gradient theory, it is necessary to determine the equilibrium densities of the coexisting phases, the chemical potentials, and the Helmholtz energy using an adequate model. For these purposes, the CPA EoS will be used in this work.

The CPA EoS was chosen because it presents several advantages over conventional cubic equations and other association models. The CPA EoS allows for an accurate description of saturated liquid densities without any need for a volume correction, in contrast to what succeeds with traditional cubic EoS, and is also mathematically simpler than other association EoSs, such as the statistical associating fluid theory (SAFT). Considering biodiesel-industry-related systems, of interest for this work, it was previously shown that the CPA EoS is the most adequate model to describe the phase equilibria of different systems appearing during the biodiesel production, purification, and use, which are characterized by containing polar compounds with strong associative interactions, taking into account its accuracy, range of applicability, simplicity, and predictive character.[31,46,51−54]

In the current work, the CPA EoS model combines a cubic contribution from the Soave−Redlich−Kwong (SRK) EoS with an association contribution, originally proposed by Wertheim.[55−57] Using a generalized cubic term (for the SRK approach with δ_1 and δ_2 equal to 0), the cubic and association contributions to the Helmholtz energy (A) are given by eqs 6 and 7[58]

$$A^{\mathrm{cubic}} = \frac{an}{b(\delta_2 - \delta_1)} \ln\left(\frac{1 + b\rho\delta_1}{1 + b\rho\delta_2}\right) - nRT \ln(1 - b\rho) \tag{6}$$

$$A^{\mathrm{assoc}} = RT \sum_i n_i \sum_{\mathrm{A}_i} \left[\ln(X\mathrm{A}_i) - \frac{X\mathrm{A}_i}{2} + \frac{1}{2}\right] \tag{7}$$

where i is a component index, b is the co-volume parameter, a is the energy parameter, ρ is the molar density, n_i is the number of moles of molecules of component i, n is the total number of moles, and $X\mathrm{A}_i$ is the mole fraction of component i not bonded at site A.

The pure-component energy parameter of CPA has a Soave-type reduced temperature dependency.

$$a(T) = a_0[1 + c_1(1 - \sqrt{T_r})]^2 \tag{8}$$

Esters are non-self-associating compounds, and therefore, there are only three pure compound parameters, the parameters of the physical part (a_0, c_1, and b), to be regressed simultaneously from vapor pressure and liquid density data. The CPA pure compound parameters for several ester families were already estimated in previous works.[25,31]

4. RESULTS AND DISCUSSION

The experimental surface tensions for the 10 biodiesel fuels studied here and the corresponding standard deviations are reported in Table 2. As expected, this property decreases with an increasing temperature and generally also with the level of unsaturation of the FAMEs constituting the biodiesel; i.e., at the same temperature, the rapeseed and sunflower biodiesel fuels present higher surface tensions and the soy-type biodiesel fuel presents lower surface tension.

Given the scarcity of surface tension data for biodiesel fuels, it was only possible to compare the surface tension data for the soybean and palm biodiesel fuels to those measured by Allen et al.[38] at 313.15 K. It is shown that our data are ca. 6% higher than Allen's data for this temperature. Although the comparison of only one point is not very conclusive, this error is acceptable given the differences in composition between the biodiesel fuels.

The predictive ability of the studied models was evaluated by calculating the relative deviations (RDs) between predicted and experimental surface tension data according to eq 9.

$$\mathrm{RD}\ (\%) = \frac{\gamma_{\mathrm{calc}_i} - \gamma_{\mathrm{exp}_i}}{\gamma_{\mathrm{exp}_i}} \times 100 \tag{9}$$

Afterward, the overall average relative deviation (OARD) was calculated through eq 9, where N_s is the number of systems studied and the average relative deviation (ARD) is the summation of the modulus of RD over N_p experimental data points.

$$\mathrm{OARD}\ (\%) = \frac{\sum_n \mathrm{ARD}}{N_s} \tag{10}$$

Using the parachors suggested by Allen et al.,[38] the predictions of surface tensions by the MacLeod−Sugden equation overestimate the experimental data within a 10% deviation (OARD of 7.7%), as shown in Figures 1 and 2. This approach provides better predictions of surface tension when the parachors suggested by Knotts et al.[45] are used, as seen in Figures 3 and 4. An OARD of 1.3% is obtained with this model that is not much

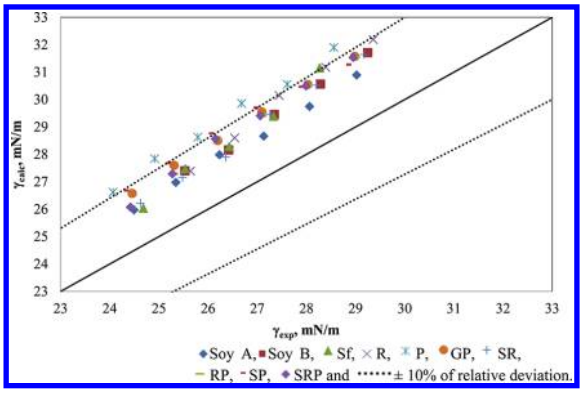

Figure 1. Linear relationship between predicted surface tensions using the MacLeod−Sugden equation with the parachors of Allen et al.[38] and experimental surface tensions equation for 10 types of pure biodiesel fuels.

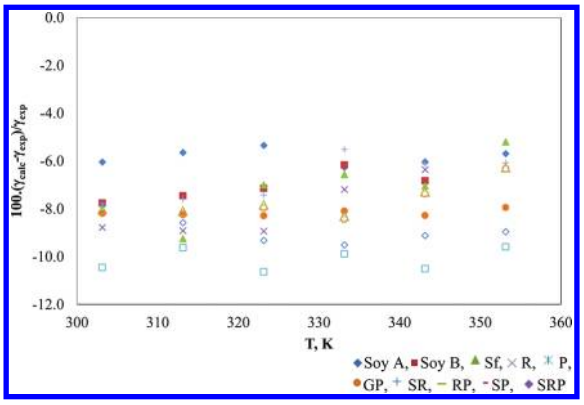

Figure 2. RDs of the predicted surface tensions obtained with the MacLeod−Sugden equation using the parachors of Allen et al.[38] as a function of the temperature for 10 biodiesel fuels.

higher than the experimental uncertainty of the data. A very good description of the temperature dependency of the experimental data is achieved using this approach, because the RDs obtained for the two versions of this model, shown in Figures 2 and 4, are almost temperature-independent. The ARDs for the 10 biodiesels studied are presented in Table 3. The reported results show the good predictive capacity of parachors through the MacLeod−Sugden equation to compute surface tensions of biodiesel fuels, in particular, when the Knotts et al.[45] parachors are used.

The gradient theory coupled with the CPA EoS was previously used for the description of the surface tensions of a series of esters, with 37 ester compounds evaluated, including formates, acetates, methyl, ethyl, propyl, butyl, and unsaturated methyl esters.[47] As discussed above, the influence parameter definition is too complex to be easily implemented, and alternatively, influence parameters are adjusted from surface tension data and plotted (far from the critical point) using the energy and covolume parameters of the physical part of the CPA EoS (as $c/ab^{2/3}$) as a function of $(1 - T_r)$.[50,59,60] It was showed in a previous work[47] that, for esters, the influence parameter dependency with the temperature is linear up to a T_r of about 0.70, and consequently, a linear approach for the influence parameter temperature dependence was considered, resulting in only two

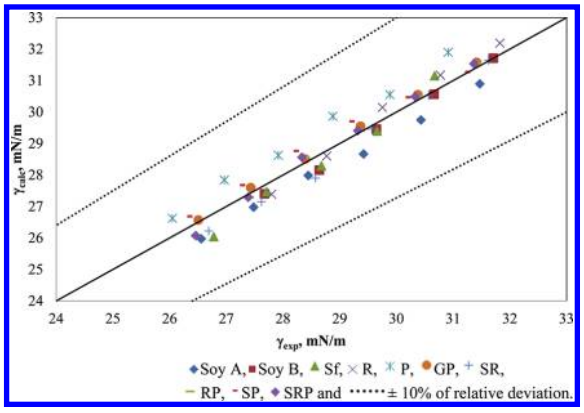

Figure 3. Linear relationship between predicted surface tensions using the MacLeod−Sugden equation with the parachors of Knotts et al.[45] and experimental surface tensions for 10 types of pure biodiesel fuels.

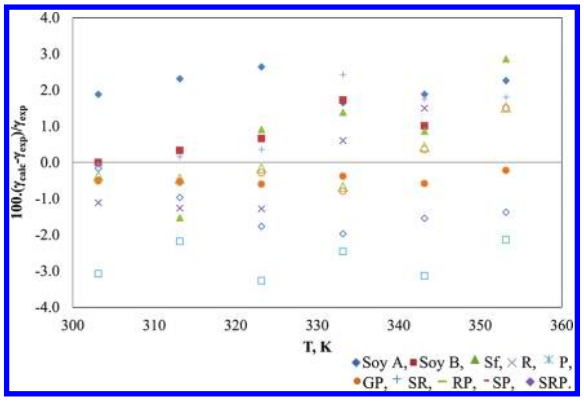

Figure 4. RDs of the predicted surface tensions obtained with the MacLeod−Sugden equation using the parachors of Knotts et al.[45] as a function of the temperature for 10 biodiesel fuels.

parameters to be correlated.

$$\frac{c}{ab^{2/3}} = D + E(1 - T_r)^2 \qquad (11)$$

Furthermore, when the parameters of the linear equation were plotted against the acentric factor, it was seen that these parameters do not vary significantly, and average values were estimated for D and E, aiming at using this approach in a predictive way, to estimate surface tensions for biodiesels. For this work, $D \times 10^6 = 0.6177$ and $E \times 10^6 = -0.4425$.[47]

Using these assumptions, the density gradient theory coupled with the CPA EoS was used to predict the surface tension data of the 10 measured biodiesels. The surface tensions are in general underpredicted and within a 10% deviation from the reported experimental data, as shown in Figure 5. The RDs are almost temperature-independent, as reported in Figure 6, showing that the temperature dependency of the experimental data is correctly described. The ARDs for the 10 biodiesels studied are presented in Table 4, and an OARD value of 9.7% was achieved.

These results are remarkable because the modeling of biodiesels with the gradient theory is considerably more difficult (and predictive) than for pure esters, because density profiles have to be calculated at each discrete point of the dividing interface limited by the upper and lower phase densities.[61] From the presented results, it is possible to conclude that the coupling of

Table 3. ARDs for Biodiesels Obtained with the MacLeod−Sugden Equation Using Allen's and Knotts' Parachors and with the Density Gradient Theory Coupled with the CPA EoS Model

	ARD (%)		
biodiesel fuels	MacLeod−Sugden equation with Allen's parachors	MacLeod−Sugden equation with Knotts'parachors	gradient theory with CPA EoS
Soy B	7.1	0.67	11
R	8.0	1.1	9.4
P	10	2.7	5.1
SR	6.6	1.3	12
PR	7.6	0.60	7.8
SP	8.9	1.3	8.2
SRP	7.7	0.66	9.6
Sf	7.0	1.5	12
GP	8.2	0.47	10
Soy A	5.8	2.1	12
OARD (%)	7.7	1.3	9.7

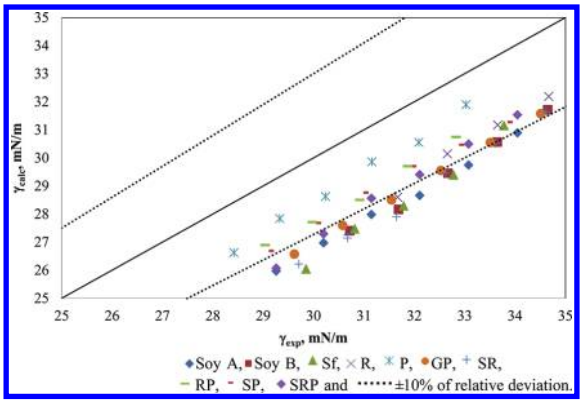

Figure 5. Linear relationship between experimental and predicted surface tensions using the density gradient theory coupled with the CPA EoS for 10 types of pure biodiesel fuels.

the gradient theory with the CPA EoS provides a more complex yet appealing approach to predict surface tensions of biodiesels, allowing for a simultaneous description of the surface tensions and phase equilibria, using constant parameters for the linear temperature dependence of the ester influence parameters. Additionally, it does not require the *a priori* knowledge of the liquid-phase densities, as occurs with the parachor models.

The surface thermodynamic properties, namely, surface entropy that corresponds to the slope of the curve of the measured surface tension data as a function of the temperature and surface enthalpy, were also determined using eqs 12 and 13.

$$S^{\gamma} = -\left(\frac{\partial \gamma}{\partial T}\right) \tag{12}$$

$$H^{\gamma} = \gamma - T\left(\frac{\partial \gamma}{\partial T}\right) \tag{13}$$

In the equation above, S^{γ} is the surface entropy in J m^{-2} K^{-1}, γ is the surface tension in mN m^{-1}, H^{γ} is the surface enthalpy in J m^{-2}, and T is the absolute temperature in K.

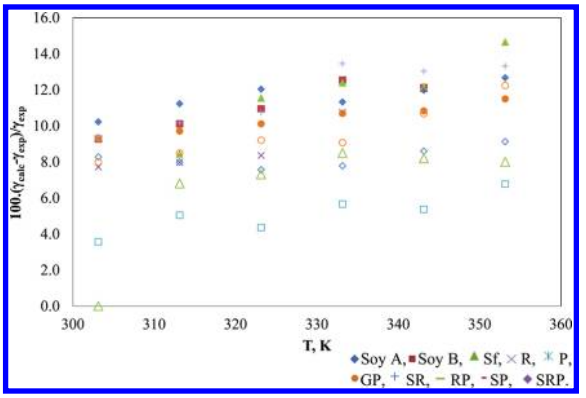

Figure 6. RDs between predicted surface tensions using the density gradient theory coupled with the CPA EoS and experimental surface tensions as a function of the temperature for 10 biodiesel fuels.

Table 4. Surface Thermodynamic Functions for the Biodiesel Fuels Studied

biodiesel	$S^{\gamma} \pm S_d$[a] ($\times 10^5$, J m^{-2} K^{-1})	$H^{\gamma} \pm S_d$ ($\times 10^2$, J m^{-2})
Soy B	10.72 ± 0.53	6.26 ± 0.17
R	12.15 ± 0.57	6.92 ± 0.18
P	10.21 ± 0.39	6.27 ± 0.13
SR	11.09 ± 0.50	6.52 ± 0.16
RP	9.69 ± 0.48	6.10 ± 0.16
SP	9.22 ± 0.10	5.93 ± 0.53
SRP	10.78 ± 0.30	6.43 ± 0.10
Sf	12.14 ± 0.87	6.89 ± 0.29
GP	9.98 ± 0.08	6.18 ± 0.03
Soy A	9.60 ± 0.30	5.99 ± 0.10

[a] S_d = expanded uncertainty with an approximate 95% level of confidence.

The values of the two surface properties and the corresponding expanded uncertainty are presented in Table 4, where it is possible to see that all of the biodiesel fuels present similar surface enthalpies but their surface entropies are dependent upon the unsaturation degree of the biodiesel. Moreover, the surface enthalpy for the biodiesel fuels is temperature-independent within the temperature range studied.

5. CONCLUSION

Surface tensions of 10 biodiesel fuels were measured at temperatures from 303.15 to 353.15 K and at atmospheric pressure.

Two different modeling approaches were used to predict the experimental data: the MacLeod−Sugden equation with two different parachor sets and the density gradient theory coupled with the CPA EoS. The first method presented an OARD of 7.7% when using the Allen's parachors and 1.3% with Knotts' parachors, showing that a simple and empirical method based on parachors can be applied to predict from the composition the temperature dependence of the biodiesel surface tensions.

Using constant parameters for the linear temperature dependence of the influence parameter for all of the fatty acid esters

constituting the different biodiesels, the gradient theory in combination with the CPA EoS was shown to predict biodiesel surface tensions with an OARD of 9.7%, while also providing information concerning the phase equilibria of the biodiesel systems.

These results clearly show that, provided that the biodiesel FAME composition is known, the predictive methods investigated here can be used to predict surface tensions of biodiesel fuels in a wide range of temperatures.

AUTHOR INFORMATION

Corresponding Author

*Telephone: +351-234401507. Fax: +351-234370084. E-mail: jcoutinho@ua.pt.

ACKNOWLEDGMENT

Samuel V. D. Freitas acknowledges funding from Fundação para a Ciência e a Tecnologia through his Ph.D. Grant SFRH/BD/51476/2011, Fundação Oriente, and the University of Aveiro. Maria Jorge Pratas acknowledges financial support from Fundação para a Ciência e a Tecnologia through her Ph.D. Grant SFRH/BD/28258/2006.

REFERENCES

(1) Demirbas, A. *Appl. Energy* **2009**, *86*, S108–S117.
(2) Gerpen, J. V. *Fuel Process. Technol.* **2005**, *86*, 1097–1107.
(3) Balat, M. *Energy Sources, Part A* **2005**, *27*, 569–577.
(4) Sharma, Y. C.; Singh, B. *Fuel* **2008**, *87*, 1740–1742.
(5) Canakci, M.; Sanli, H. *J. Ind. Microbiol. Biotechnol.* **2008**, *35*, 431–441.
(6) Lotero, E.; Liu, Y.; Lopez, D. E.; Suwannakarn, K.; Bruce, D. A.; Goodwin, J. G. *Ind. Eng. Chem. Res.* **2005**, *44*, 5353–5363.
(7) Knothe, G. *Energy Environ. Sci.* **2009**, *2*, 759–766.
(8) Demirbas, A. *Energy Sources, Part A* **2008**, *30*, 1830–1834.
(9) Joshi, R. M.; Pegg, M. J. *Fuel* **2007**, *86*, 143–151.
(10) Knothe, G. *Energy Fuels* **2010**, *24*, 2098–2103.
(11) Anand, K.; Ranjan, A.; Mehta, P. S. *Energy Fuels* **2009**, *24*, 664–672.
(12) Demirbas, A. *Energy Sources, Part A* **2010**, *32*, 628–636.
(13) Kerschbaum, S.; Rinke, G. *Fuel* **2004**, *83*, 287–291.
(14) Zhang, Y.; Dube, M. A.; McLean, D. D.; Kates, M. *Bioresour. Technol.* **2003**, *89*, 1–16.
(15) Phan, A. N.; Phan, T. M. *Fuel* **2008**, *87*, 3490–3496.
(16) Anand, K.; Sharma, R. P.; Mehta, P. S. *Appl. Therm. Eng.* **2011**, *31*, 235–242.
(17) Alptekin, E.; Canakci, M. *Fuel* **2009**, *88*, 75–80.
(18) Moser, B. *In Vitro Cell. Dev. Biol.: Plant* **2009**, *45*, 229–266.
(19) Benjumea, P.; Agudelo, J.; Agudelo, A. *Fuel* **2008**, *87*, 2069–2075.
(20) Saka, S.; Kusdiana, D. *Fuel* **2001**, *80*, 225–231.
(21) Leung, D. Y. C.; Wu, X.; Leung, M. K. H. *Appl. Energy* **2010**, *87*, 1083–1095.
(22) American Society for Testing and Materials (ASTM). *ASTM D6751-09 Standard Specification for Biodiesel Fuel Blend Stock (B100) for Middle Distillate Fuels*; ASTM: West Conshohocken, PA, 2009.
(23) European Committee for Standardization (CEN). *BS EN 14214 Automotive Fuels: Fatty Acid Methyl Esters (FAME) for Diesel Engines: Requirements and Test Methods*; CEN: Brussels, Belgium, 2009.
(24) Pratas, M. J.; Freitas, S. V. D.; Oliveira, M. B.; Monteiro, S. C.; Lima, A. S.; Coutinho, J. A. P. *Energy Fuels* **2011**, *25*, 2333–2340.
(25) Pratas, M. J.; Gallego, M. J. P.-.; Oliveira, M. B.; Queimada, A. J.; Piñeiro, M. M.; Coutinho, J. A. P. *Energy Fuels* **2011**.
(26) Pratas, M. J.; Oliveira, M. B.; Pastoriza-Gallego, M. J.; Queimada, A. J.; Piñeiro, M. M.; Coutinho, J. A. P. *Energy Fuels* **2011**, *25*, 3806–3814.
(27) Ceriani, R.; Gonçalves, C. B.; Coutinho, J. A. P. *Energy Fuels* **2011**, *25*, 3712–3717.
(28) Freitas, S. V. D.; Pratas, M. J.; Ceriani, R.; Lima, A. S.; Coutinho, J. A. P. *Energy Fuels* **2010**, *25*, 352–358.
(29) Pratas, M. J.; Freitas, S.; Oliveira, M. B.; Monteiro, S. C.; Lima, A. S.; Coutinho, J. A. P. *J. Chem. Eng. Data* **2010**, *55*, 3983–3990.
(30) Freitas, S. V.; Pratas, M. J.; Silva, S. M.; Lima, A. S.; Coutinho, J. A. P. *Energy Fuels* **2011**.
(31) Oliveira, M. B.; Varanda, F. R.; Marrucho, I. M.; Queimada, A. J.; Coutinho, J. A. P. *Ind. Eng. Chem. Res.* **2008**, *47*, 4278–4285.
(32) Costa, M. B.; Boros, L. A. D.; Coutinho, J. A. P.; Krähenbühl, M. A.; Meirelles, A. J. A. *Energy Fuels* **2011**, *25*, 3244–3250.
(33) Coutinho, J. A. P.; Goncalves, M.; Pratas, M. J.; Batista, M. L. S.; Fernandes, V. F. S.; Pauly, J.; Daridon, J. L. *Energy Fuels* **2010**, *24*, 2667–2674.
(34) Boros, L.; Batista, M. L. S.; Vaz, R. V.; Figueiredo, B. R.; Fernandes, V. F. S.; Costa, M. C.; Krähenbühl, M. A.; Meirelles, A. J. A.; Coutinho, J. A. P. *Energy Fuels* **2009**, *23*, 4625–4629.
(35) Lopes, J. C. A.; Boros, L.; Krähenbühl, M. A.; Meirelles, A. J. A.; Daridon, J. L.; Pauly, J.; Marrucho, I. M.; Coutinho, J. A. P. *Energy Fuels* **2007**, *22*, 747–752.
(36) Ejim, C. E.; Fleck, B. A.; Amirfazli, A. *Fuel* **2007**, *86*, 1534–1544.
(37) Shu, Q.; Wang, J.; Peng, B.; Wang, D.; Wang, G. *Fuel* **2008**, *87*, 3586–3590.
(38) Allen, C.; Watts, K.; Ackman, R. *J. Am. Oil Chem. Soc.* **1999**, *76*, 317–323.
(39) Rolo, L. I.; Caço, A. I.; Queimada, A. J.; Marrucho, I. M.; Coutinho, J. A. P. *J. Chem. Eng. Data* **2002**, *47*, 1442–1445.
(40) Queimada, A. J.; Silva, F. A. E.; Caço, A. I.; Marrucho, I. M.; Coutinho, J. A. P. *Fluid Phase Equilib.* **2003**, *214*, 211–221.
(41) Freire, M. G.; Carvalho, P. J.; Queimada, A. J.; Marrucho, I. M.; Coutinho, J. A. P. *J. Chem. Eng. Data* **2006**, *51*, 1820–1824.
(42) Carvalho, P. J.; Neves, C. M. S. S.; Coutinho, J. A. P. *J. Chem. Eng. Data* **2010**, *55*, 3807–3812.
(43) Carvalho, P. J.; Freire, M. G.; Marrucho, I. M.; Queimada, A. J.; Coutinho, J. A. P. *J. Chem. Eng. Data* **2008**, *53*, 1346–1350.
(44) Freire, M. G.; Carvalho, P. J.; Fernandes, A. M.; Marrucho, I. M.; Queimada, A. J.; Coutinho, J. A. P. *J. Colloid Interface Sci.* **2007**, *314*, 621–630.
(45) Knotts, T. A.; Wilding, W. V.; Oscarson, J. L.; Rowley, R. L. *J. Chem. Eng. Data* **2001**, *46*, 1007–1012.
(46) Oliveira, M. B.; Queimada, A. J.; Coutinho, J. A. P. *Ind. Eng. Chem. Res.* **2009**, *49*, 1419–1427.
(47) Oliveira, M. B.; Coutinho, J. A. P.; Queimada, A. J. *Fluid Phase Equilib.* **2011**, *303*, 56–61.
(48) Oliveira, M. B.; Marrucho, I. M.; Coutinho, J. A. P.; Queimada, A. J. *Fluid Phase Equilib.* **2008**, *267*, 83–91.
(49) Miqueu, C.; Mendiboure, B.; Graciaa, A.; Lachaise, J. *Ind. Eng. Chem. Res.* **2005**, *44*, 3321–3329.
(50) Queimada, A. J.; Miqueu, C.; Marrucho, I. M.; Kontogeorgis, G. M.; Coutinho, J. A. P. *Fluid Phase Equilib.* **2005**, *228*−*229*, 479–485.
(51) Oliveira, M. B.; Miguel, S. I.; Queimada, A. J.; Coutinho, J. A. P. *Ind. Eng. Chem. Res.* **2010**, *49*, 3452–3458.
(52) Oliveira, M. B.; Pratas, M. J.; Marrucho, I. M.; Queimada, A. J.; Coutinho, J. A. P. *AIChE J.* **2009**, *55*, 1604–1613.
(53) Oliveira, M. B.; Queimada, A. J.; Coutinho, J. A. P. *J. Supercrit. Fluids* **2010**, *52*, 241–248.
(54) Oliveira, M. B.; Teles, A. R. R.; Queimada, A. J.; Coutinho, J. A. P. *Fluid Phase Equilib.* **2009**, *280*, 22–29.
(55) Kontogeorgis, G. M.; Michelsen, M. L.; Folas, G. K.; Derawi, S.; Von Solms, N.; Stenby, E. H. *Ind. Eng. Chem. Res.* **2006**, *45*, 4855–4868.
(56) Kontogeorgis, G. M.; Michelsen, M. L.; Folas, G. K.; Derawi, S.; Von Solms, N.; Stenby, E. H. *Ind. Eng. Chem. Res.* **2006**, *45*, 4869–4878.
(57) Oliveira, M. B.; Coutinho, J. A. P.; Queimada, A. J. *Fluid Phase Equilib.* **2007**, *258*, 58–66.

(58) Queimada, A. J.; Mota, F. L.; Pinho, S. P.; Macedo, E. A. *J. Phys. Chem. B* **2009**, *113*, 3469–3476.
(59) Cornelisse, P. M. W.; Peters, C. J.; de Swaan Arons, J. *Fluid Phase Equilib.* **1993**, *82*, 119–129.
(60) Miqueu, C.; Mendiboure, B.; Graciaa, A.; Lachaise, J. *Fluid Phase Equilib.* **2003**, *207*, 225–246.
(61) Miqueu, C.; Mendiboure, B.; Graciaa, A.; Lachaise, J. *Ind. Eng. Chem. Res.* **2005**, *44*, 3321–3329.